

Spatiotemporal analysis of precipitation trends during 1961–2010 in Hubei province, central China

Ranghui Wang · Cheng Li

Received: 11 October 2014 / Accepted: 26 February 2015 / Published online: 14 March 2015
© Springer-Verlag Wien 2015

Abstract Precipitation is an important climatic parameter, and its variability severely affects regional hydrological processes and water resource management. In order to explore the changing spatial and temporal characteristics of precipitation-related indices, including precipitation amounts indices, extreme precipitation indices, and precipitation concentration indices, in Hubei province, central China during 1961–2010, several precipitation-related indices series were analyzed using the Mann-Kendall test, Pettitt test, and inverse distance weighted interpolation method in this paper. The results are as follows: (1) A clear south–north gradient is apparent in the spatial distribution of the majority of precipitation-related indices, while the distribution of other indices (i.e., CDD, PCD, and PCP) is just the opposite. Most part of Hubei province can experience mixed positive and negative trends in precipitation-related indices. (2) The majority of precipitation-related indices exhibit an increasing trend, but most of which are not significant. July has the largest positive trend, with a regional average of 14.76 mm/decade. As for extreme precipitation indices, there exist large variations in Hubei, especially in R95pTOT. Besides, no obvious trends are shown in precipitation concentration indices. (3) With the exception of consecutive dry days (CDD), most of extreme precipitation indices are strongly correlated with annual mean precipitation (AMP) in Hubei. And the extreme precipitation indices are well correlated with each other except CDD and consecutive wet days (CWD). For six precipitation-related

indices (i.e., SDII, RX1day, RX5day, R95pTOT, R99pTOT, and PCD), there are significant positive relationships with Northern Hemisphere Subtropical High (NHS) but significant negative relationships with Northern Hemisphere Polar Vortex (NHPV). Furthermore, the majority of precipitation-related indices have significant negative correlations with East Asian summer monsoon index (EASMI) and South China Sea summer monsoon index (SCSSMI), and the correlation coefficient with EASMI is higher than that with SCSSMI.

1 Introduction

With rapid population growth and economic development, global climate change has attracted much attention. The Fourth Assessment Report of IPCC (2007) indicated that the global mean annual temperature had increased by 0.74 °C during the past 100 years. The global warming not only directly affects the variation in temperature extremes but also leads to aggravation in the frequency and intensity of extreme events, e.g., drought, flood, heat wave, rainstorm, etc., which have caused enormous economic losses and exerted a negative impact on agricultural production activities, and water resource management (Dash et al. 2012; Gaffin et al. 2004). These extreme events had a close relation with the spatiotemporal distribution of precipitation (Xu et al. 2005). At the same time, precipitation is also one of the most important meteorological elements for detecting and diagnosing regional climate change. Thus, several precipitation-related indices, e.g., precipitation amounts indices, extreme precipitation indices, and precipitation concentration indices, are widely used by many researchers to analyze the variation characteristics of precipitation in various regions.

Generally speaking, the global land annual precipitation has significantly increased by about 2 % in the 20th century

R. Wang
School of Environmental Science and Engineering, Nanjing
University of Information Science and Technology, Nanjing 210044,
China

C. Li (✉)
School of Geography and Remote Sensing, Nanjing University of
Information Science and Technology, Nanjing 210044, China
e-mail: lichengnuist@163.com

(Jones and Hulme 1996). However, different regions presented different trends. Dore (2005) pointed out that annual land precipitation has continued to increase in the arid and semi-arid region of Asia, Australia, northern half of Europe, northwestern Mexico, subtropical Argentina, Paraguay, Brazil, North America, Arctic, northeast Pacific region, and source region of Antarctic intermediate water, while decreasing trends have been observed in the boreal Asia, temperate Asia, southern Europe, southwest Pacific region, and tropical Africa. Besides, no obvious trend in annual precipitation has been reported over the tropical Asia, Colombia, and Japan (Klein Tank et al. 2006; Xu et al. 2003). Zhai et al. (2005) found that there are distinctive regional and seasonal patterns of precipitation trends in China. The annual mean precipitation has decreased significantly in central, northern, and northeastern China but has increased significantly in southwestern, northwestern, and eastern parts of the country (Wang and Zhou 2005). Relevant results indicated that the uneven distribution of precipitation in space and time was very obvious in most river basins of China, which could be experiencing serious meteorological disasters (Becker et al. 2008; Jiang et al. 2006).

New analyses showed that in regions where total precipitation has increased, it is very likely that there have been even more pronounced increases in heavy and extreme precipitation events (Dore 2005; Zhang et al. 2005). In China, heavy and extreme events have slightly increased although annual total precipitation has decreased (Alexander et al. 2006; You et al. 2011), and Zhang et al. (2011) also indicated that increasing fractional contribution of shorter consecutive wet days may imply intensifying precipitation. However, different regions in China exhibited different trends in previous studies. Observations showed that extreme precipitation increased in the mid-lower reaches of the Yangtze River basin (Su et al. 2006), southeast (Fischer et al. 2012) and some regions in northwestern China (Jiang et al. 2013), while the decreasing trends of extreme precipitation were investigated in the northeast and southwest regions of China (Zhai et al. 2005; Li et al. 2012). Abrupt changes of the number of days with extreme precipitation and the percentage of extreme precipitation were found in the end of 1970s and the beginning of 1980s over China (Zhang et al. 2008).

Higher precipitation concentration, represented not only by higher percentages of the annual total precipitation in a few very rainy days but also by the time and degree of concentration of the yearly total precipitation within a year, has the potential to cause floods and droughts (Li et al. 2011b). The occurrence of droughts and floods has displayed an increasing trend since the 1990s, especially in the bigger river basins over China (Bai and Liu 2010; Gemmer et al. 2008). Moreover, the changes in spatial and temporal concentration degree and variation of heavy precipitation were the major possible reasons for the frequent flood disasters (Xie et al. 2005). At present,

three different types of indices, including precipitation concentration index (CI), precipitation concentration degree (PCD), and precipitation concentration period (PCP), have been used to detect the precipitation concentration in some regions. Martin-Vide (2004) presented the CI to evaluate the contribution of the days of greatest rainfall to the total amount in Peninsular Spain. Similarly, PCI could also be used in the changing properties of precipitation concentration in China, e.g., the Pearl River basin (Zhang et al. 2009), Xinjiang (Li et al. 2011b). Besides, Zhang and Qian (2003) proposed that the knowledge of calculating the PCD and PCP based on vector of daily precipitation. Bai and Liu (2010) investigated the features of rainfall variation over east China, indicating that the PCD and PCP were helpful to analyze the temporal and spatial characteristic of drought-flood disasters.

Located in the mid-lower reaches of the Yangtze River basin, Hubei is a major producer of grain in central China with abundant water resources, which display an important role in the economic development, and eco-environment conservation. The study region is expected to be sensitive and susceptible to climate warming due to complex underlying surfaces and terrain (Wang et al. 2014). Although a few studies have been conducted on the precipitation changes in the Yangtze River basin (Jiang et al. 2006; Becker et al. 2008), the analysis of precipitation concentration in the Yangtze River basin reported in the literature was very limited. It is particularly true for Hubei province. Moreover, a majority of previous studies have concentrated on the second half of the twentieth century, and the recent years have not been included. Thus, the major objectives of this study were to detect long-term trends of precipitation-related indices in both space and time based on historically observed daily precipitation data during 1961–2010 and investigate the correlations of these indices. The detailed analysis and understanding of variation characteristics of precipitation in Hubei may reduce the climate-induced drought-flood disasters and provide a useful reference for water resource management.

2 Study region and data

2.1 Study region

Hubei province (29°05′–33°20′ N, 108°21′–116°07′ E), with the total population of more than 61 million, is located in the mid-lower reaches of the Yangtze River basin and to the north of the Dongting Lake. Taking Wuhan as the capital city, Hubei covers an area of approximately 1.86×10^5 km², which is the fourteenth largest province of China, and has three diverse topographic zones, including the mountain, plain, and hill, with an elevation ranging from 2995 to 12 m. The regional climate is of the subtropical monsoon type, which is characterized by abundant precipitation and high temperatures from

June to August. The mean annual precipitation is 800 to 1600 mm, and the average annual temperature is 12.1 to 17.9 °C.

Hubei has an important and unique position in central China. On the one hand, it is one of the main grain-producing areas in China, with two largest agricultural bases, e.g., Jiangnan Plain and North Hillock. Some major agricultural products take an important place all over the country. On the other hand, the water resources in Hubei are abundant. The province has a dense hydrological network, thus winning the title “A Province with One Thousand Lakes”. At present, there are over 4000 large and small rivers, totaling over 60,000 km long.

Nature hazards, such as severe droughts and frequent floods, have caused serious losses to the agriculture and hindered economic development. Due to subtropical monsoon climate and topography, the spatiotemporal distribution of precipitation is uneven, with 72 % of the annual total precipitation concentrated from April to September. Some reports suggested that summer was the main flooding season in the Yangtze River basin (Huang et al. 2014). Jiang and Wen (2007) pointed out that drought-flood disasters occurred almost every year in Hubei.

2.2 Data

The daily precipitation data used in this paper covers the period from 1961 to 2010. It was collected from 35 national meteorological observing stations in Hubei and was provided by the National Climate Center (NCC) of China Meteorological Administration (CMA). Before calculating and analyzing the precipitation indices, the missing data would be processed by simple linear correlation between its neighboring stations. Meanwhile, it was necessary to do the quality control and homogeneity assessment detection of the dataset based on the software package RclimDex (<http://etccdi.pacificclimate.org/software.shtml>) and the software package RHtests V3 (<http://ccma.seos.uvic.ca/ETCCDI>).

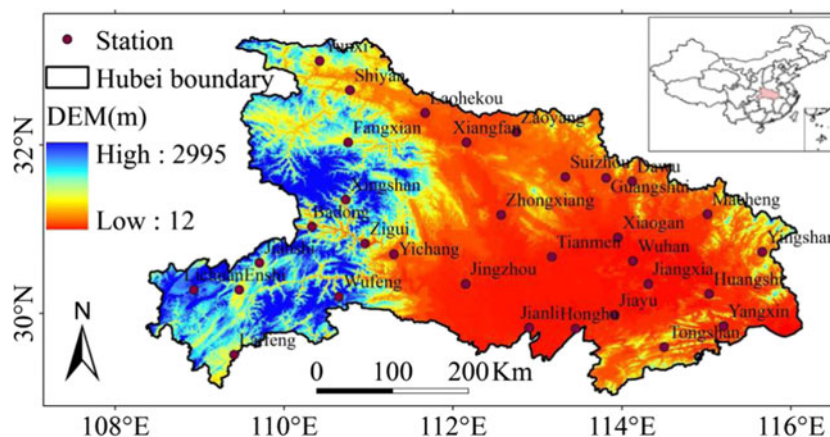
After rejecting three stations with inhomogeneous series of daily precipitation, 32 stations were finally selected in this paper. The locations of the 32 stations are plotted in Fig. 1.

The historical drought-flood disaster data over Hubei province was collated from various sources including China Meteorological Disaster Encyclopedia (Volume of Hubei) (Jiang and Wen 2007) and Yearbook of Meteorological Disasters in China (ECYMDC 2005–2010), which were published by the Meteorological Press of CMA. These data contain the monitoring information about drought-flood disasters, e.g., the time and site of generation; the intensity and duration of disasters; the affected population, area and agricultural region, and direct economic losses associated with disasters.

Large-scale atmospheric circulation indices selected in this paper, which could include Northern Hemisphere Subtropical High (NHSH) (5° E–360°) and Northern Hemisphere Polar Vortex (NHPV) (0–360°), were provided by the NCC of CMA. The annual data spanned over the years between 1961 and 2010. Based on previous studies (Fischer et al. 2012; Liang et al. 2015), NHSH could be divided into three parts: North Africa-Atlantic-North America Subtropical High (NAANASH) (110° W–60° E), India Subtropical High (ISH) (65° E–95° E), and Pacific Subtropical High (PSH) (110° E–115° W). Similarly, NHPV could be divided into four parts: Asia Polar Vortex (APV) (60° E–150° E), Pacific Polar Vortex (PPV) (150° E–120° W), North America Polar Vortex (NAPV) (120° W–30° W), and Atlantic European Polar Vortex (AEPV) (30° W–60° E).

The East Asian Summer Monsoon index (EASMI) is based on the intensity of the normalized seasonality of the wind field at 850 hPa (10°–40° N, 110°–140° E) for June to August (Li and Zeng 2003). Similarly, the South China Sea summer monsoon index (SCSSMI) is based on the intensity of the normalized seasonality of the wind field at 925 hPa (0°–25° N, 100°–125° E) for June to September (Li and Zeng 2003). The annual EASMI and SCSSMI data was available on the website (<http://ljp.lasg.ac.cn/dct/page/65540>).

Fig. 1 Meteorological stations used in this study and location of Hubei Province



2.3 Methodology

In this study, the temporal trends and spatial distributions of precipitation-related indices in Hubei during 1961–2010 are examined by the Mann-Kendall trend test and calculated by Kendall slope estimator. Abrupt change points in an observed time series of precipitation are detected by the Pettitt test. Meanwhile, in order to better understand the features of precipitation, the spatial distribution patterns are employed to draw using inverse distance weighted (IDW) interpolation method based on ArcGIS9.3 software package in this paper. The principles of calculating indices and methods are described in detail as follows:

2.3.1 Extreme precipitation indices

The ETCCDI defined 27 core extreme indices based on daily temperature and precipitation data, which had relatively weak extreme, low noise and strong significances that can reflect the change of extreme climate in different aspects (Wang et al. 2014). Relevant exact definitions of all the indices are available from the ETCCDI website (<http://cccma.seos.uvic.ca/ETCCDMI>). In this study, 12 extreme precipitation indices are listed in Table 1. These indices were usually divided into three types, i.e., frequency indices, intensity indices, and percentile-based indices. An R-language program, RClimDexV3, developed at the Climate Research Branch of the Meteorological Service of Canada and available from the ETCCDI web site, is applied to calculate these extreme indices.

2.3.2 Mann-Kendall (M-K) trend test

The non-parametric Mann-Kendall (M-K) statistical test (Mann 1945; Kendall 1975), which is a rank-based procedure, is frequently applied to characterize the trends in climate data series (Huang et al. 2013). In this study, the M-K test is used to analyze the trends for precipitation-related indices and to test their significance.

In the M-K test, the test statistic is calculated as follows:

$$S = \sum_{i=1}^{n-1} \sum_{j=i+1}^n \text{sgn}(x_j - x_i) \tag{1}$$

where

$$\text{sgn}(x_j - x_i) = \begin{cases} +1, & x_j > x_i \\ 0, & x_j = x_i \\ -1, & x_j < x_i \end{cases} \tag{2}$$

In Eqs. 1 and 2, x_j and x_i are the sequential data values, and n is the number of data points. The statistic S is approximately

Table 1 Definitions of the 12 selected extreme precipitation indices

Indices	Description	Units
PRCPTOT	Annual total precipitation in wet days	mm
SDII	Annual total precipitation divided by the number of wet days in the year	mm/day
RX1day	Annual maximum 1-day precipitation	mm
RX5day	Annual maximum consecutive 5-day precipitation	mm
R95pTOT	Annual precipitation due to very wet days when RR >95th percentile of 1961–1990 daily rainfall	mm
R99pTOT	Annual precipitation due to extremely wet days when RR >99th percentile of 1961–1990 daily rainfall	mm
NW	Annual count of days when RR ≥ 1 mm	days
R10mm	Annual count of days when RR ≥ 10 mm	days
R20mm	Annual count of days when RR ≥ 20 mm	days
R30mm	Annual count of days when RR ≥ 30 mm	days
CDD	Maximum number of consecutive days with RR < 1 mm	days
CWD	Maximum number of consecutive days with RR ≥ 1 mm	days

Let RR be the daily precipitation amount on a wet day. Moreover, 30 mm was the threshold defined by the authors

normally distributed when $n \geq 8$, with the mean and the variance as formula (Eq. 3) and (Eq. 4):

$$E(S) = 0 \tag{3}$$

$$V(S) = \frac{n(n-1)(2n+5) - \sum_{i=1}^n t_i i(i-1)(2i+5)}{18} \tag{4}$$

In Eq. 4, n is the number of data points, and t_i denotes the number of ties of extent i . The standard normal test statistic Z is computed by using Eq. (5):

$$Z = \begin{cases} \frac{s-1}{\sqrt{\text{Var}(s)}}, & S > 0 \\ 0, & S = 0 \\ \frac{s-1}{\sqrt{\text{Var}(s)}}, & S < 0 \end{cases} \tag{5}$$

Positive Z values denote increasing trends, and negative Z values show decreasing trends while zero Z values indicate no change trends. Testing trends are done at the specific significance level ($\alpha = 10\%$). When $|Z| > 1.645$, the null hypothesis of no trend is rejected and a significant trend exists in the time.

At the same time, another very useful index is the Kendall slope, which is the magnitude of the monotonic change (You et al. 2011) and is given as follows:

$$\beta = \text{Median} \left(\frac{x_j - x_i}{j - i} \right), \forall j < i, \quad 1 \leq i \leq n \tag{6}$$

In Eq. 6, the unbiased estimator β is the median overall combination of record pairs for the whole data.

2.3.3 Detection of abrupt climatic change

Pettitt test proved to be powerful and as for a useful tool for exploring the abrupt change points in a long-term trend analysis (Du et al. 2013). The non-parametric Pettitt (1979) test, which detects a shift in the mean at an unknown time, and calculates its statistical significance, is used to identify the significant change point in the observed time series of precipitation in this paper.

The Pettitt test considers a sequence of random variables and divides it into two groups represented by $x_1; x_2; \dots; x_t$ and $x_{t+1}; x_{t+2}; \dots; x_n$. If each group has a common distribution function, then the change point is identified at t . In order to achieve the identification of change point, a statistical index $U_{t,n}$ is expressed as follows:

$$U_{t,n} = \sum_{i=1}^t \sum_{j=t+1}^n \text{sgn}(x_i - x_j), 1 \leq t \leq n \tag{7}$$

where similar to the M-K test,

$$\text{sgn}(x_j - x_i) = \begin{cases} +1, & x_j > x_i \\ 0, & x_j = x_i \\ -1, & x_j < x_i \end{cases} \tag{8}$$

The most probable change point is found where its value is:

$$k_t = \max_{1 \leq t \leq n} |U_{t,n}| \tag{9}$$

and the significance probability associated with value K_t is evaluated as

$$\rho = 2 \exp\left(\frac{-6k_t^2}{n^3 + n^2}\right) \tag{10}$$

If ρ is smaller than the specific significance level in Eq. 10, the null hypothesis is rejected. In other words, if a significant change point exists, the time series is divided into two parts at the location of the change point t . The approximate significance probability for a change point is defined as $p = 1 - \rho$. In this study, the specific significance level is at the 90 % confidence level.

2.3.4 Precipitation concentration indices

Two types of precipitation concentration indices, including precipitation concentration degree (PCD) and precipitation concentration period (PCP), are used to represent the changing features of precipitation concentration and discuss the basic characteristics of drought-flood disasters and their formation

mechanism in Hubei. Specially, PCD can correctly reflect the precipitation concentration level during the certain period in a year, and PCP may indicate in which month the maximal rain appears during a year (Li et al. 2011b). According to the new definitions of PCD and PCP (Zhang and Qian 2003), they can quantitatively characterize the spatiotemporal heterogeneity of the precipitation. The basic principle for calculating PCD and PCP is based on vector analysis (Xie et al. 2005). The assumption can be made that precipitation values are vector quantities with both magnitude and direction. One year is considered as a cycle (360°) and then 1 month is corresponding to 30°. The monthly precipitation amount can be viewed as the length of vector, whereas the angle corresponding to the mid-month of each year is taken as the vector direction. Table 2 gives one scheme of defining the angle value in this paper.

The main steps can be calculated as follows:

$$R_x = \sum_{i=1}^{12} r_{xi} = \sum_{i=1}^{12} r_i \sin \theta_i \tag{11}$$

$$R_y = \sum_{i=1}^{12} r_{yi} = \sum_{i=1}^{12} r_i \cos \theta_i \tag{12}$$

In Eqs. 11 and 12, r_i is the monthly precipitation amount, and θ_i is the representative angle of the corresponding month.

Hence, the total synthetic and PCD are respectively defined by

$$R = \sqrt{R_x^2 + R_y^2} = \sqrt{\sum_{i=1}^{12} (r_i \sin \theta_i)^2 + \sum_{i=1}^{12} (r_i \cos \theta_i)^2} \tag{13}$$

$$PCD = \frac{R}{R_i} = \frac{\sqrt{\sum_{i=1}^{12} (r_i \sin \theta_i)^2 + \sum_{i=1}^{12} (r_i \cos \theta_i)^2}}{\sum_{i=1}^{12} r_i} \tag{14}$$

Table 2 The angle range of each month precipitation vector and the mid-month angle

Month	Angle range (°)	Mid-month angle (°)	Month	Angle range (°)	Mid-month angle (°)
Jan	345–15	0	Jul	165–195	180
Feb	15–45	30	Aug	195–225	210
Mar	45–75	60	Sep	225–255	240
Apr	75–105	90	Oct	255–285	270
May	105–135	120	Nov	285–315	300
Jun	135–165	150	Dec	315–345	330

In Eq. 14, R_i is the annual total precipitation amount.

As the ratio of the synthetic component in horizontal to the synthetic component in vertical is the tangent of the vector angle, PCP is calculated as follows:

$$PCP = \arctan\left(\frac{R_x}{R_y}\right) \quad (15)$$

The unit of PCP is degree, and the corresponding relationship between angle value and the months can be seen in the Table 2.

3 Results and analysis

3.1 Spatial distribution for the M-K test and mean values of precipitation-related indices

The spatial distribution for the M-K test and mean values of monthly and annual precipitation series at each individual station in Hubei during 1961–2010 are given in Fig. 2. It can be seen from Fig. 2 that the monthly mean precipitations (MMP) are the largest or dominant in July, ranging between

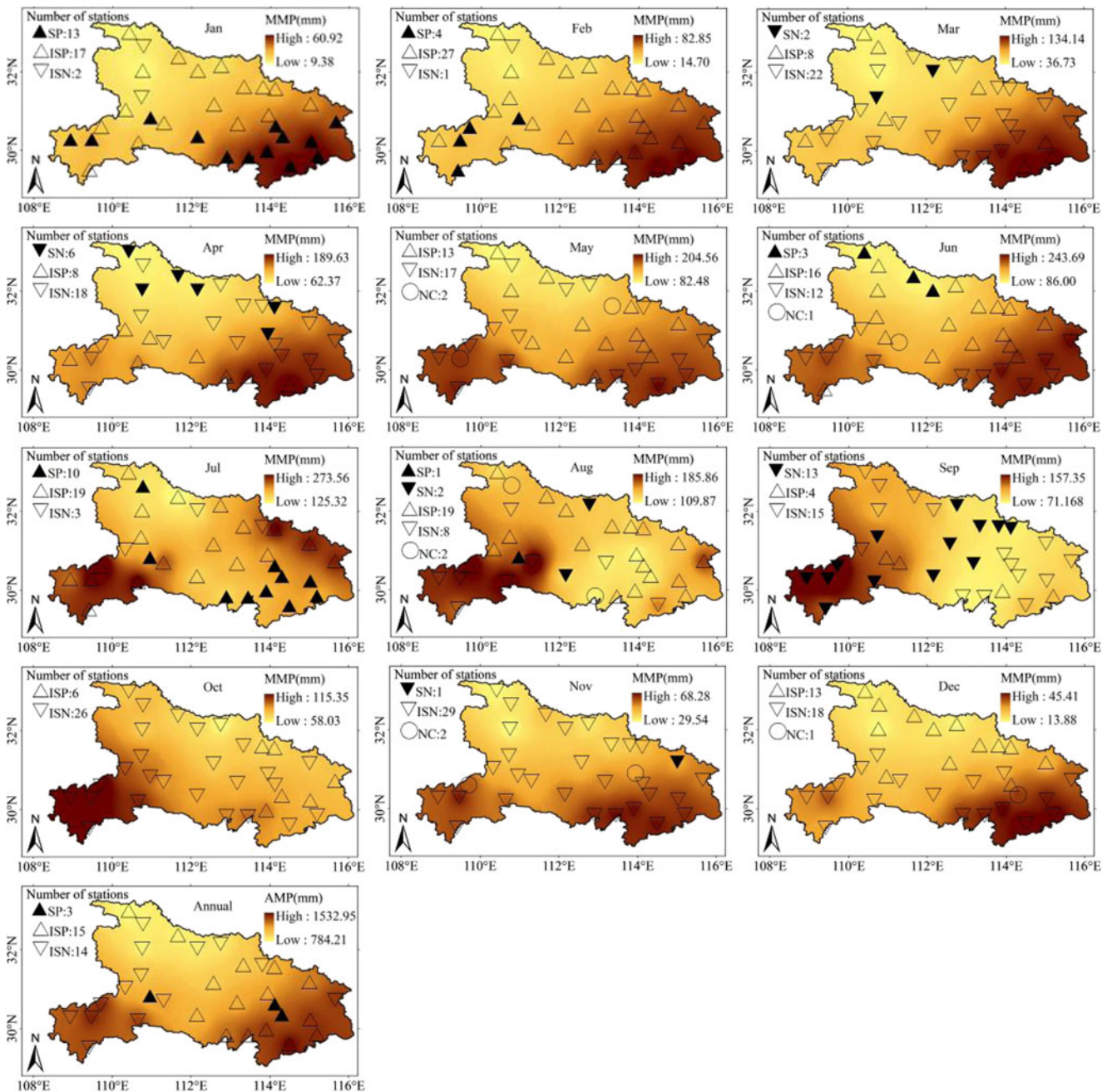


Fig. 2 Spatial distribution for M-K trends and mean values of monthly and annual precipitation during 1961–2010 (the legend in the left corner is used to indicate the number of stations with significant positive (SP),

insignificant positive (ISP), significant negative (SN), insignificant negative (ISN), and no change (NC) trends)

125.32 and 273.56 mm, while the lowest MMP occur in December, varying from 13.88 to 45.41 mm. MMP in 12 months present four different spatial distribution features. Firstly, in January, February, March, April, and December, MMP show a decreasing trend from southeast to northwest, that is, wetting in southeastern but drying in northwest area. Secondly, MMP in May, June, and November demonstrate an obvious decreasing tendency from south to north. Thirdly, MMP during the months of August, September, and October exhibit a decreasing trend from northwest to southeast. Last but not the least, there are two high-value areas with MMP for July in southwestern and northeastern Hubei. As for the annual mean precipitation (AMP), AMP ranges from 1532.95 to 784.21 mm, gradually decreasing from south to north.

In addition, Fig. 2 also illustrates the number of stations with different trends of monthly and annual precipitation series for each individual station. It can be seen that January has

the largest number of stations showing significant increasing trends with 13 stations, which are mainly located in the south-east of Hubei. July ranks the second largest with ten stations. However, the largest number of stations indicating significant decreasing trends occurs in September with 16 stations, followed by April with six stations, which are found in the northern area of the province. As for annual patterns, the number of stations with increasing AMP is slightly more than that of stations with decreasing AMP. However, the number of stations characterized by statistically significant increasing AMP is only three, accounting for 9.38 % of the total stations analyzed.

The mean values of 12 extreme precipitation indices present three different spatial distribution features (Fig. 3). Firstly, the mean values of the mean precipitation amount on a wet day (SDII) show a decreasing tendency from southeast to northwest, varying from 14.22 to 9.34 mm/day. Secondly,

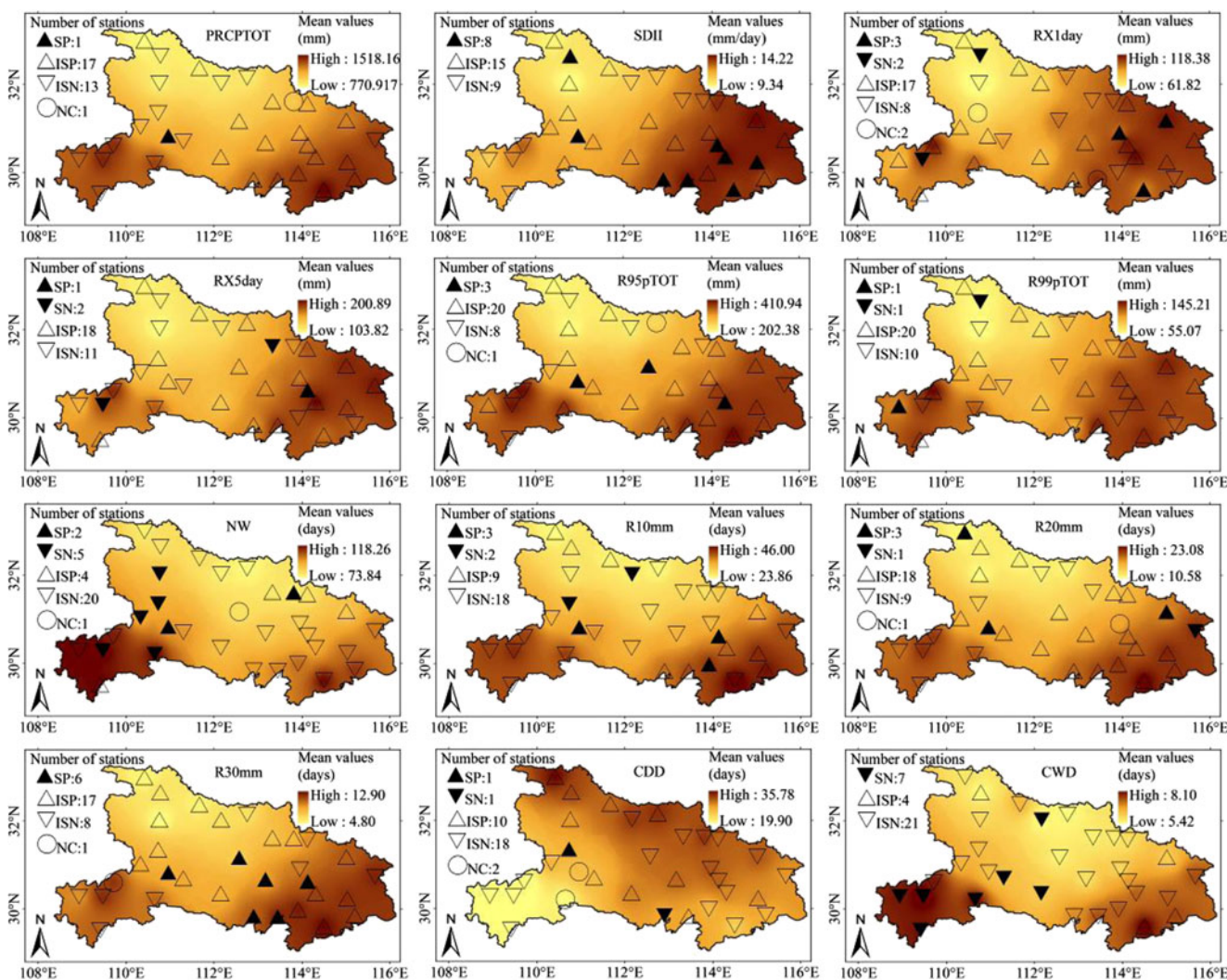


Fig. 3 Spatial distribution for M-K trends and mean values of 12 extreme precipitation indices during 1961–2010 (the legend in the left corner is used to indicate the number of stations with significant positive (SP),

insignificant positive (ISP), significant negative (SN), insignificant negative (ISN), and no change (NC) trends)

the mean values of the consecutive dry days (CDD) demonstrate an obvious decreasing trend from north to south, ranging between 19.90 and 35.78 days/decade, especially part of high-value areas are mainly located in the middle-top regions between 112° E and 114° E. Last but not the least, the mean values in the rest of extreme precipitation indices, e.g., the wet day precipitation (PRCPTOT), the maximum 1-day precipitation (RX1DAY), the very wet day precipitation (R95pTOT), the wet days (NW), etc., exhibit a decreasing tendency from south to north, with two high-value areas located in southwestern and southeastern Hubei. Under the influence of relevant factors, e.g., precipitation, terrain, eco-environment, etc., the drought-flood disasters occur frequently in recent years (Su et al. 2006). The increasing AMP mainly results from increasing heavy rain or rainstorm, while the unbalanced spatial and temporal distribution of precipitation can play an important role in the formation of drought-flood disasters (Huang et al. 2014).

As shown in Fig. 3, SDII has the largest number of stations showing significant increasing trends with eight stations, which are mainly located in the southeastern Hubei. The occurrence of extremely heavy precipitation days (R30mm) ranks the second largest with 12 stations, which are found in the regions between 110° E and 114° E. The occurrence of heavy precipitation days (R10mm) and very heavy precipitation days (R20mm) as well as R95pTOT rank the third largest. However, the maximum number of consecutive wet days (CWD) has the largest number of stations showing significant decreasing trends with 13 stations, which are mainly found in the southwestern of Hubei.

The mean values of PCD in Hubei range from 33.36 to 46.86 %, which are larger than those of the southeast China but lower than those of the north part of China (Bai and Liu 2010). And the high-value areas in Hubei are mainly located in the regions between 109° E and 111° E (Fig. 4). It is shown

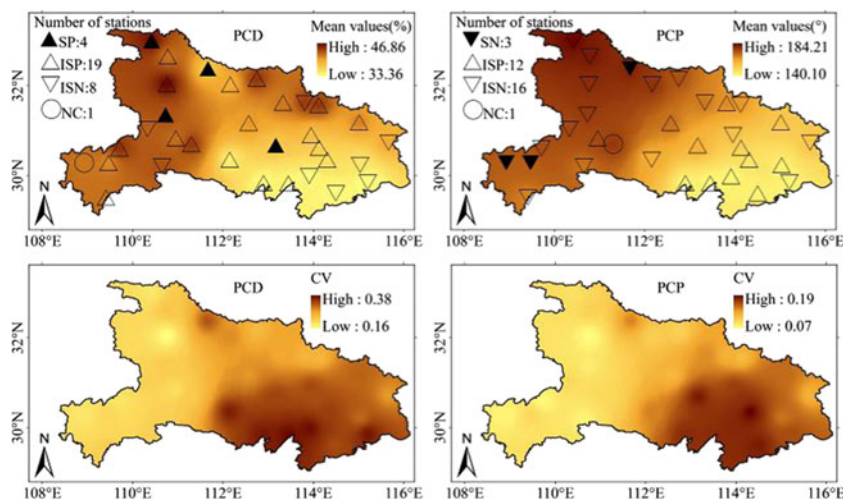
in Fig. 4 and Table 2 that the time of PCP approximately appears from the beginning of June to the middle of July, which are latter than those of the southeast China but earlier than those of the north part of China (Bai and Liu 2010). PCP occurs earliest in the southeastern region of Hubei, while it occurs latest in the western mountain region of the province. On the whole, the movement of the rain belt may be considered as the important reason for the changes of PCD and PCP. Zhang and Qian (2003) found that the longer the rainy reason is or the more the rainy seasons are there, the smaller the value of PCD will be and vice versa. The PCP appears in May for the first time in the Southeast China, and the gradient of the PCP in the reaches of Yangtze River is rather great. With the increase of latitudes, the appearance of PCP is loitering from the end of July to the beginning of August in the reaches of Yellow River. According to Fig. 4, the coefficients of variation of PCD and PCP denote a decreasing trend from southeast to northwest, which may reflect that both have the similar distribution, and the major center of variation may exist in the southeastern Hubei.

As seen in Fig. 4, the stations with significant increasing trends for PCP are mainly located in the northwestern regions of the province. When it comes to PCP, the significant decreasing trends are found in the regions between 109° E and 112° E.

3.2 Regional trends and change points detection analysis of precipitation-related indices

In order to understand the statistical characteristics of precipitation on the different time scales, the monthly and annual precipitation series over entire Hubei province are calculated by using arithmetic mean method based on observed precipitation data of all the stations during 1961–2010. The M-K test and the Kendall slope estimator in the regional precipitation are used to explore the variation trend and the trend rate,

Fig. 4 Spatial distribution for M-K trends, mean values, and coefficients of variation (CV) of PCD and PCP during 1961–2010 (the legend in the left corner is used to indicate the number of stations with significant positive (SP), insignificant positive (ISP), significant negative (SN), insignificant negative (ISN), and no change (NC) trends)



respectively (Table 3). As shown in Table 3, the precipitation over entire Hubei province shows statistically significant increasing trends for January and July, while precipitation in autumn presents a significant decreasing trend during 1961–2010. Their Kendall slopes are 3.16, 14.76, and -11.4 mm/decade, respectively. The largest trend rate of precipitation is in summer, varying from -8.68 to 47.96 mm/decade, with a regional average of 15.10 mm/decade. On the whole, the trend rate of annual precipitation is 3.86 mm/decade, showing a slightly increasing tendency. However, Wang and Zhou (2005) pointed out that annual mean precipitation has decreased significantly in central China. And the trends of annual precipitation have reached -5.4 mm/decade in the mid-lower reaches of the Yangtze River basin (Li et al. 2013). Compared with the studies in the Yangtze River basin and China, the different results in this paper may indicate that the variation of precipitation has relatively obvious regional characteristics.

The abrupt changes of the precipitation data time series in this study are used to detect by using the Pettitt method. Table 3 also lists these change points in different time scales and the approximate significance probability p for the corresponding change point. According to Table 3, the change points of January, February, March, September, and October occur in the late 1970s, and the results of January and September are statistically significant. Concerning annual precipitation, there is no significant change point found over the past 50 years in Hubei. Fischer et al. (2012) denoted that there were large differences in the direction and time for climate jump of precipitation in China; however, no change points in annual total precipitation were estimated. Ding and Zhang (2008) indicated that no sudden changes were detected

for annual, spring, and winter precipitation during 1961–2006 in the Yangtze River basin.

As seen in Table 4, the extremely wet day precipitation (R99pTOT) and the maximum 5-day precipitation (RX5DAY) over the entire Hubei province experience statistically significant increasing trends, and their slopes are 7.27 and 1.69 mm/decade, respectively. CWD displays a significant decreasing tendency, with a regional average of -0.20 days/decade. When it comes to other extreme precipitation indices, most of them display insignificant increasing trends. Thus, there is a tendency towards increasing trends dominating, consistent with the intensification of the hydrological cycle in Hubei. The largest trend rate of extreme precipitation indices is R95pTOT, varying from -14.68 to 39.34 mm/decade, with a regional average of 12.77 mm/decade. Moreover, You et al. (2011) pointed out that the regional trends of PRCPTOT, SDII, RX1day, RX5day, CDD, and R95pTOT in China reached 3.21 mm/decade, 0.06 mm/decade, 1.37 mm/decade, 1.90 mm/decade, -1.22 days/decade, and 4.06 mm/decade, respectively. Wang et al. (2008) demonstrated that the SDII, R95pTOT, and R99pTOT could present a significant positive tendency in the mid-lower reaches of the Yangtze River basin, with the regional trends of 0.27 , 0.24 , and 0.24 mm/10a, respectively. Compared with the studies in the Yangtze River basin and China, the extreme precipitation indices in Hubei have large variations as a whole.

The change points of RX5day, NW, R10mm, and CDD appear in the late 1980s, while that of other extreme precipitation indices occur in the 1970s, except for R20mm (Table 4). In addition, the result of CWD is statistically significant at the confidence level of 90 %.

Table 3 The M-K test and Pettitt test for monthly and annual precipitation over entire Hubei province

	M-K test				Pettitt test		
	Z values	Trends	Kendall slope (mm/decade)	Range (mm/decade)	Change point (year)	K_T	p
Jan	2.23	Positive	3.16	-1.32 to 8.19	1986	-284	0.02
Feb	1.18	Positive	3.34	-0.36 to 6.41	1987	-199	0.16
Mar	-0.67	Negative	-1.87	-3.84 to 1.89	1993	147	0.36
Apr	-0.37	Negative	-1.34	-8.20 to 3.78	1977	133	0.43
May	-0.27	Negative	-0.87	-6.96 to 9.15	1978	104	0.60
Jun	0.22	Positive	1.01	-17.23 to 13.13	1978	-144	0.38
Jul	1.66	Positive	14.76	-3.46 to 27.70	1978	-202	0.15
Aug	0.12	Positive	1.17	-10.85 to 19.28	1965	113	0.55
Sep	-1.52	Negative	-6.49	-23.56 to 3.78	1989	227	0.08
Oct	-0.62	Negative	-2.28	-5.86 to 5.45	1987	123	0.49
Nov	-0.47	Negative	-1.55	-5.69 to -0.15	1967	111	0.56
Dec	0.03	Positive	0.07	-2.00 to 1.72	1979	87	0.70
Annual	0.33	Positive	3.86	-43.35 to 54.25	1979	-69	0.80

Results in bold type indicate statistically significant at the 10 % significance level

Table 4 The M-K test and Pettitt test for extreme precipitation indices over entire Hubei province

	M-K test				Pettitt test		
	Z values	Trends	Kendall slope	Range	Change point (year)	K_T	p
PRCPTOT	0.32	Positive	4.39 (mm/decade)	-41.40 to 54.84 (mm/decade)	1979	-73	0.78
SDII	1.15	Positive	0.18 (mm/decade)	-0.21 to 0.50 (mm/decade)	1978	-166	0.27
RX1day	1.02	Positive	1.58 (mm/decade)	-8.19 to 8.22 (mm/decade)	1978	-148	0.36
RX5day	1.92	Positive	1.69 (mm/decade)	-12.10 to 13.42 (mm/decade)	1993	-115	0.54
R95pTOT	1.39	Positive	12.77 (mm/decade)	-14.68 to 39.34 (mm/decade)	1978	-168	0.26
R99pTOT	1.66	Positive	7.27 (mm/decade)	-1.00 to 12.87 (mm/decade)	1978	-168	0.26
NW	-0.95	Negative	-0.85 (days/decade)	-3.33 to 2.11 (days/decade)	2003	159	0.30
R10mm	-0.49	Negative	-0.20 (days/decade)	-1.08 to 1.30 (days/decade)	1993	77	0.76
R20mm	0.60	Positive	0.17 (days/decade)	-0.73 to 0.91 (days/decade)	1966	-63	0.83
R30mm	1.16	Positive	0.23 (days/decade)	-0.40 to 0.95 (days/decade)	1978	-118	0.52
CDD	-0.13	Negative	-0.08 (days/decade)	-1.48 to 1.67 (days/decade)	1999	99	0.63
CWD	-1.79	Negative	-0.20 (days/decade)	-0.69 to 0 (days/decade)	1974	226	0.09

Results in bold type indicate statistically significant at the 10 % significance level

According to Table 5, PCD over entire Hubei province experiences an increasing trend, and the slope is 0.60 %/decade. PCP denotes a decreasing tendency, with a regional average of -0.12°/decade. However, no abrupt changes of PCD and PCP are detected using the Pettitt method.

3.3 Correlations analysis of annual precipitation and extreme precipitation indices

The principal component analysis of the precipitation data displays that the cumulative contribution of two principal components can reach 82.78 %, and its eigenvalue is greater than 2.18, which meet the requirements of subsequent analysis (Table 6). As shown in Table 6, the first factor (F1) explains 65.95 % of the overall variance, which may denote the similarity of variations in AMP over entire Hubei province and extreme precipitation indices. And the load values of extreme precipitation indices are generally large, except for that of CDD and CWD. The variance ratio contribution of the second factor (F2) is about 16.83 %, including NW, CWD, R10mm, and CDD, and their load values can be up to 0.82, 0.60, 0.52, and -0.59, respectively. According to Table 7, the correlations between AMP over entire Hubei province and extreme precipitation indices are obviously significant at the 99 % confidence level except CDD, with correlation coefficients higher

than 0.66, suggesting that extreme precipitation indices are strongly correlated with AMP. Meanwhile, there are statistically significant correlations among the extreme precipitation indices at the 95 % confidence level except CDD and CWD. You et al. (2011) indicated that extreme precipitation events were positively correlated with annual total precipitation. The results in this study are in agreement with the findings of previous work in China.

3.4 Correlations analysis between precipitation-related indices and large-scale atmospheric circulation indices, summer monsoon indices

The relationships between precipitation-related indices and the NASH index, NHPV index are shown in Tables 8 and 9, respectively. As for six indices (i.e., SDII, RX1day, RX5day, R95pTOT, R99pTOT, and PCD), there are significant positive relationships with NASH, while there exist significant negative relationships with NHPV, which can indicate that when NASH is strong or NHPV is weak, the intensity of extreme precipitation events may increase, and vice versa (Liang et al. 2015). Moreover, NAANASH has the more significant impacts on the six indices. Similarly, the relationship between the six indices and APV is the strongest. At the same time, the majority of precipitation-related indices have significant

Table 5 The M-K test and Pettitt test for PCD and PCP over entire Hubei province

	M-K test				Pettitt test		
	Z values	Trends	Kendall slope	Range	Change point (year)	K_T	p
PCD	1.51	Positive	0.60 (%/decade)	-1.20 to 2.16 (%/decade)	1978	-120	0.51
PCP	-0.09	Negative	-0.12 (°/decade)	-4.31 to 2.85 (°/decade)	1979	-121	0.50

Table 6 Factor loadings of the variance of AMP and extreme precipitation indices

Factors	AMP	PRCPTOT	SDII	RX1 day	RX5 day	R95pTOT	R99pTOT	NW	R10 mm	R20 mm	R30mm	CDD	CWD	% Variance
F1	0.97	0.97	0.88	0.86	0.86	0.94	0.90	0.48	0.81	0.94	0.94	0.25	0.22	65.95
F2	0.22	0.22	-0.40	-0.25	-0.16	-0.29	-0.29	0.82	0.52	0.11	-0.11	-0.59	0.60	16.83

negative correlations with EASMI and SCSSMI (Table 10), and the correlation coefficient with EASMI is higher than that with SCSSMI, which can denote that EASM is one of the main factors affecting the variation of the regional precipitation. The similar result has been reported in the previous work (Yu et al. 2004; Wang and Zhou 2005). Li et al. (2011a) found that when EASM was stronger (weaker) than normal, the Yangtze River basin and regions south of it were prone to drought (flood) after the 1920s.

4 Discussions and conclusions

4.1 Discussions

With the frequent occurrence of drought-flood disasters, precipitation-related indices have attracted more and more attention recently (Gemmer et al. 2008; Li et al. 2011b; Huang et al. 2013). The majority of precipitation-related indices present a positive trend, especially in the extreme precipitation indices. Compared with previous studies in global (Alexander et al. 2006), China (You et al. 2011), central and south Asia (Klein Tank et al. 2006), western central Africa (Aguilar et al. 2009), Middle East (Zhang et al. 2005), central and northern south America (Aguilar et al. 2005), the intensity of extreme precipitation indices in Hubei have large

variations, which reflect that the intensity of precipitation tends to increase. Meanwhile, some extreme precipitation indices, e.g., SDII, RX1d, and RX5d, in the Yangtze River basin would all increase at different degrees in the future (Huang et al. 2012). Changes in precipitation extremes are likely to enhance intensity of drought-flood disasters (Su et al. 2006; Gemmer et al. 2008), which can bring with negative effects on the eco-environment conservation and agricultural production activities. Research results of this paper indicate that southeastern Hubei is a potential risk-prone region. Therefore, the relevant effective measures should be taken to prevent and reduce drought-flood disasters due to extreme precipitation events in Hubei province.

The changes in large-scale atmospheric circulations and monsoon activities display an important role in the regional precipitation. Fischer et al. (2012) indicated that East Asia summer monsoon was one of the key elements of the climate system and strongly affected precipitation changes in most regions of China. Si et al. (2009) found that the movement of the rain belt in the Yangtze River basin was closely related to the advance and retreat of East Asia summer monsoon. Specially, summer monsoon advances to the Yangtze River basin in mid-June during the meiyu period. Thus, the summer precipitation increased in the mid-lower reaches of the Yangtze River basin (Huang et al. 2014). Furthermore, Zhang et al. (2011) indicated that anomalies of atmospheric

Table 7 Pearson’s correlation coefficients between AMP and extreme precipitation indices for Hubei province

	AMP	PRCPTOT	SDII	RX1 day	RX5 day	R95pTOT	R99pTOT	NW	R10 mm	R20 mm	R30mm	CDD	CWD
AMP	1												
PRCPTOT	0.77**	1											
SDII	0.74**	0.77**	1										
RX1day	0.75**	0.74**	0.79**	1									
RX5day	0.85**	0.75**	0.75**	0.90**	1								
R95pTOT	0.85**	0.85**	0.94**	0.88**	0.84**	1							
R99pTOT	0.78**	0.78**	0.86*	0.96**	0.91**	0.94**	1						
NW	0.66**	0.66**	0.03	0.24	0.30*	0.21	0.22	1					
R10mm	0.92**	0.92**	0.54**	0.48**	0.53**	0.59**	0.51**	0.81**	1				
R20mm	0.96**	0.96**	0.83**	0.69**	0.69**	0.84**	0.73**	0.52**	0.87**	1			
R30mm	0.91**	0.91**	0.92**	0.73**	0.72**	0.91**	0.79**	0.33**	0.74**	0.95**	1		
CDD	0.13	0.13	0.44**	0.21	0.23	0.39**	0.29*	-0.32*	-0.05	0.20	0.32	1	
CWD	0.28*	0.28*	-0.05	0.07	0.19	0.04	0.06	0.50**	0.39**	0.19	0.08	-0.01	1

*Significant at the 0.05 level; **significant at the 0.01 level

Table 8 Pearson's correlation coefficients between precipitation-related indices and Northern Hemisphere Subtropical High

	Area of NHSH	Strength of NHSH	Area of NAAN ASH	Strength of NAAN ASH	Area of ISH	Strength of ISH	Area of PSH	Strength of PSH
AMP	0.22	0.26	0.25	0.28*	0.21	0.29*	0.18	0.20
PRCPTOT	0.23	0.27	0.26	0.29*	0.21	0.29*	0.18	0.20
SDII	0.40**	0.44**	0.43**	0.45**	0.20	0.27	0.36*	0.37**
RX1day	0.33*	0.38**	0.37**	0.42**	0.16	0.23	0.28*	0.28
RX5day	0.25	0.30*	0.27	0.33*	0.15	0.22	0.21	0.23
R95pTOT	0.35*	0.39**	0.39**	0.42**	0.17	0.25	0.30*	0.31*
R99pTOT	0.34*	0.39**	0.38**	0.42**	0.17	0.23	0.30*	0.30*
NW	-0.13	-0.11	-0.12	-0.10	0.10	0.12	-0.15	-0.13
R10mm	0.11	0.14	0.12	0.15	0.25	0.31*	0.07	0.09
R20mm	0.27	0.32*	0.30*	0.33*	0.21	0.29*	0.23	0.27
R30mm	0.33*	0.37**	0.37**	0.38**	0.18	0.27	0.29*	0.32*
CDD	0.07	0.05	-0.01	0.01	-0.02	0.12	0.13	0.13
CWD	-0.22	-0.18	-0.28*	-0.21	-0.08	-0.02	-0.16	-0.13
PCD	0.32*	0.35*	0.31*	0.32*	0.09	0.14	0.33*	0.37**
PCP	-0.04	-0.02	0.01	0.01	-0.09	-0.12	-0.07	-0.05

*Significant at the 0.05 level; **significant at the 0.01 level

circulations could be the important reasons for the variability of the intensity and frequency of extreme precipitation in China. Relevant research results revealed that significant correlations could be detected between the heavy rainfall in the Yangtze River basin and another large-scale atmospheric circulations, including Arctic oscillation (AO), Antarctic oscillation (AAO), North Atlantic oscillation (NAO), Indian summer monsoon (ISM), Pacific North American pattern (PNA)

(Jiang et al. 2006; Sun et al. 2009; Gong et al. 2011; Zhao et al. 2011; Sundaram et al. 2012). These results reflect the complexity of regional precipitation change, but the detailed mechanisms still need the future works.

In order to explore the relationship between AMP and drought-flood disasters over Hubei province, the high-value years and the low-value years of AMP, PCD, PCP as well as the drought-flood years are listed in Table 11. According to

Table 9 Pearson's correlation coefficients between precipitation-related indices and Northern Hemisphere Polar Vortex

	Area of NHPV	Strength of NHPV	Area of APV	Strength of APV	Area of PPV	Strength of PPV	Area of NAPV	Strength of NAPV	Area of AEPV	Strength of AEPV
AMP	-0.24	-0.22	-0.26	-0.21	-0.13	-0.15	-0.10	-0.14	-0.23	-0.14
PRCPTOT	-0.24	-0.22	-0.27	-0.21	-0.13	-0.15	-0.10	-0.15	-0.24	-0.15
SDII	-0.29*	-0.39**	-0.40**	-0.26	-0.05	-0.21	-0.28*	-0.37**	-0.19	-0.21
RX1day	-0.30*	-0.39**	-0.37**	-0.33*	-0.10	-0.21	-0.21	-0.31*	-0.24	-0.25
RX5day	-0.20	-0.35*	-0.32*	-0.21	-0.06	-0.20	-0.06	-0.31*	-0.17	-0.25
R95pTOT	-0.30*	-0.36**	-0.39**	-0.29*	-0.07	-0.15	-0.28*	-0.35*	-0.21	-0.20
R99pTOT	-0.31*	-0.40**	-0.40**	-0.34*	-0.06	-0.15	-0.26	-0.37**	-0.25	-0.27
NW	-0.03	0.12	0.07	-0.03	-0.16	-0.02	0.19	0.24	-0.13	0.02
R10mm	-0.14	-0.06	-0.14	-0.07	-0.13	-0.11	0.03	0.03	-0.16	-0.06
R20mm	-0.26	-0.27	-0.29*	-0.23	-0.12	-0.20	-0.14	-0.19	-0.26	-0.16
R30mm	-0.29*	-0.33*	-0.34*	-0.26	-0.10	-0.20	-0.21	-0.28*	-0.25	-0.18
CDD	-0.12	-0.10	-0.12	-0.07	0.13	0.09	-0.34*	-0.26	-0.08	0.08
CWD	0.17	0.10	0.19	0.03	0.16	0.15	0.23	0.06	0.01	0.02
PCD	-0.05	-0.28	-0.25	-0.17	0.18	0.02	-0.14	0.41**	0.01	-0.12
PCP	-0.01	-0.16	-0.01	-0.14	0.01	-0.02	-0.01	-0.23	-0.01	-0.02

*Significant at the 0.05 level; **significant at the 0.01 level

Table 10 Pearson’s correlation coefficients between precipitation-related indices and EASMI, SCSSMI

	EASMI	SCSSMI
AMP	-0.42**	-0.31**
PRCPTOT	-0.43**	-0.31**
SDII	-0.55**	-0.48**
RX1day	-0.37**	-0.31**
RX5day	-0.38**	-0.33**
R95pTOT	-0.54**	-0.43**
R99pTOT	-0.46**	-0.40**
NW	0.01	0.10
R10mm	-0.30**	-0.16
R20mm	-0.46**	-0.39**
R30mm	-0.53**	-0.47**
CDD	-0.24	-0.24
CWD	0.02	0.01
PCD	-0.57**	-0.51**
PCP	-0.05	-0.19

**Significant at the 0.01 level

Table 11, higher values of AMP or PCD are likely to lead to severe floods, while the region suffers from severe droughts in the lower values of AMP or PCD. Zhang and Qian (2003) found that though AMP has a certain relationship with droughts and floods, it is not the direct and sole cause. Huang et al. (2013) pointed out that the precipitation tends to concentrate in the flood season, which can increase the rainfall effectively and result in less droughts. When the PCD is too low, the precipitation process disperses, especially in the flood season, making the incidence of drought probably higher (Bai and Liu 2010). Moreover, if PCP is early, it is likely that droughts occur in the region, while late PCP can possibly result in drought-flood disasters. Thus, the three elements interact with each other in such a way that they have an important impact on the formation of drought-flood disasters in Hubei. So, the drought-flood disaster early warning and improvement of disaster prevention and mitigation capability is a serious problem that Hubei province has to face.

Table 11 The distribution of years with extreme precipitation and drought-flood disasters over entire Hubei province

Type	High-value years					
AMP	1983	1989	1998	1980	1996	1969
PCD	1979	1980	1969	1998	1983	1991
PCP	<i>2000</i>	1983	<i>1981</i>	1996	2008	1965
Type	Low-value years					
AMP	1966	<i>2001</i>	<i>1978</i>	<i>1976</i>	2006	<i>1992</i>
PCD	<i>1972</i>	<i>2001</i>	<i>1981</i>	<i>1961</i>	1993	1989
PCP	<i>1990</i>	2009	<i>1992</i>	2002	<i>1966</i>	2007

Results in bold type indicate the floods, while slanted numerals denote the droughts

4.2 Conclusions

The spatial and temporal characteristics of several precipitation-related indices during the period of 1961 to 2010 in Hubei province were explored in this paper. The main findings are summarized as follows:

1. A clear south–north gradient was apparent in the spatial distribution of the majority of precipitation-related indices, while the distribution of other indices (i.e., CDD, PCD, and PCP) was just the opposite. Most part of the Hubei province could experience mixed positive and negative trends in precipitation-related indices. January had more than ten stations presenting significant increasing trends, and July ranked the second largest, which were mainly located in the southeastern Hubei. However, April had the largest number of stations showing significant decreasing trends with six stations, which were found in the middle and western areas of Hubei province.
2. The majority of precipitation-related indices exhibited an increasing trend, but most of which were not significant. July had the largest positive trend, with a regional average of 14.76 mm/decade, in monthly and annual precipitation. For the regional average trends of precipitation extremes, NW, R10mm, CDD, and CWD presented decreasing trends, while other indices showed increasing trends, and RX5day, R99pTOT, CWD were statistically significant. The largest trend rate of extreme precipitation indices was R95pTOT, with a regional average of 12.77 mm/decade. Besides, PCD and PCP had weak and insignificant trends.
3. With the exception of CDD, most of extreme precipitation indices were strongly correlated with AMP in Hubei. Meanwhile, the extreme precipitation indices were well correlated with each other except CDD and CWD. For the six precipitation-related indices (i.e., SDII, RX1day, RX5day, R95pTOT, R99pTOT, and PCD), there were significant positive relationships with NNSH, while there existed significant negative relationships with NHPV. Specially, NAANASH and APV had the more significant impacts on the six indices. Furthermore, a majority of precipitation-related indices had significant negative correlations with EASMI and SCSSMI, and the correlation coefficient with EASMI was higher than that with SCSSMI.

Acknowledgments This paper was financially supported by the National Key Technology R&D Program of China (No. 2012BAC23B01, 2012BAD16B0305), and the National 973 Program of China (No. 2006CB705809). We would like to thank the NCC of CMA for providing valuable climate datasets. The authors would like to thank Dr. Huang, NUIST, and other reviewers for their invaluable suggestions, which are helpful for improving the quality of our paper.

References

- Aguilar E, Peterson TC, Obando PR et al (2005) Changes in precipitation and temperature extremes in Central America and northern South America, 1961–2003. *J Geophys Res* 110, D23107. doi:10.1029/2005JD006119
- Aguilar E, Barry AA, Brunet M et al (2009) Changes in temperature and precipitation extremes in western central Africa, Guinea Conakry, and Zimbabwe, 1955–2006. *J Geophys Res* 114, D02115. doi:10.1029/2008JD011010
- Alexander LV, Zhang X, Peterson TC et al (2006) Global observed changes in daily climate extremes of temperature and precipitation. *J Geophys Res* 111, D05109. doi:10.1029/2005JD006290
- Bai AJ, Liu XD (2010) Characteristics of rainfall variation over East China for the last 50 years and their relationship with droughts and floods. *J Trop Meteor* 16(3):255–262
- Becker S, Hartmann H, Zhang Q, Wu Y, Jiang T (2008) Cyclicity analysis of precipitation regimes in the Yangtze River basin, China. *Int J Climatol* 28(5):579–588. doi:10.1002/joc.1572
- Dash SK, Sharma N, Pattayak KC, Gao XJ, Shi Y (2012) Temperature and precipitation changes in the north-east India and their future projections. *Glob Planet Chang* 98–99:31–44
- Ding YH, Zhang L (2008) Inter-comparison of the time for climate abrupt change between the Tibetan Plateau and other regions in China. *Chin J Atmos Sci* 32(4):794–780 (in Chinese)
- Dore MHJ (2005) Climate change and changes in global precipitation patterns: what do we know? *Environ Int* 31:1167–1181
- Du J, Fang J, Xu W, Shi PJ (2013) Analysis of dry/wet conditions using the standardized precipitation index and its potential usefulness for drought/flood monitoring in Hunan Province, China. *Stoch Environ Res Risk Assess* 27(2):377–387
- Fischer T, Gemmer M, Liu L, Su BD (2012) Change-points in climate extremes in the Zhujiang River Basin, South China, 1961–2007. *Clim Chang* 110:783–799
- Gaffin SR, Rosenzweig C, Xing X, Yetman G (2004) Downscaling and geo-spatial gridding of socio-economic projections from the IPCC special report on emissions scenarios (SRES). *Glob Environ Chang* 14(2):105–123
- Gemmer M, Jiang T, Su BD, Kundzewicz ZW (2008) Seasonal precipitation changes in the wet season and their influence on flood/drought hazards in the Yangtze River Basin, China. *Quat Int* 186:12–21
- Gong DY, Yang J, Kim SJ, Gao YQ, Guo D, Zhou TJ, Hu M (2011) Spring Arctic Oscillation-East Asian summer monsoon connection through circulation changes over the western North Pacific. *Clim Dynam* 37(11–12):2199–2216
- Huang J, Zhang JC, Zhang ZX, Sun SL, Yao J (2012) Simulation of extreme precipitation indices in the Yangtze River basin by using statistical downscaling method (SDSM). *Theor Appl Climatol* 108(3–4):325–343
- Huang J, Sun SL, Zhang JC (2013) Detection of trends in precipitation during 1960–2008 in Jiangxi province, southeast China. *Theor Appl Climatol* 114(1–2):237–251
- Huang J, Sun SL, Xue Y, Zhang JC (2014) Spatial and temporal variability of precipitation indices during 1961–2010 in Hunan Province, central south China. *Theor Appl Climatol* 118(3):581–595
- IPCC (2007) The fourth assessment report: climate change 2007. Cambridge University Press, New York
- Jiang HR, Wen KG (2007) Chinese meteorological disasters ceremony (Hubei volume). China Meteorological Press, Beijing (in Chinese)
- Jiang T, Zhang Q, Zhu DM, Wu YJ (2006) Yangtze floods and droughts (China) and teleconnections with ENSO activities. *Quatern Int* 144(1):29–37
- Jiang FQ, Hu RJ, Wang SP, Zhang YW, Tong L (2013) Trends of precipitation extremes during 1960–2008 in Xinjiang, the Northwest China. *Theor Appl Climatol* 111(1–2):133–148
- Jones PD, Hulme M (1996) Calculating regional climatic time series for temperature and precipitation: methods and illustrations. *J Climatol* 16:361–377
- Kendall MG (1975) Rank correlation methods. Griffin, London
- Klein Tank AMG, Peterson TC, Quadir DA et al (2006) Changes in daily temperature and precipitation extremes in central and south Asia. *J Geophys Res* 111, D16105. doi:10.1029/2005JD006316
- Li JP, Zeng QC (2003) A new monsoon index and the geographical distribution of the global monsoons. *Adv Atmos Sci* 20(2):299–302
- Li Q, Wei FY, Li DL (2011a) Interdecadal variation of East Asian summer monsoon and drought/flood distribution over eastern China in the last 159 years. *J Geogr Sci* 21(4):579–593
- Li XM, Jiang FQ, Li LH, Wang GG (2011b) Spatial and temporal variability of precipitation concentration index, concentration degree and concentration period in Xinjiang, China. *Int J Climatol* 31(11):1679–1693. doi:10.1002/joc.2181
- Li ZX, He YQ, Theakstone WH, Wang XF, Wei Z, Cao WH, Du JK, Xin HJ, Chang L (2012) Altitude dependency of trends of daily climate extremes in southwestern China, 1961–2008. *J Geogr Sci* 22(3):416–430
- Li CL, Zhang FW, Zi L, Yan FH (2013) Analysis on variation features of multi-years precipitation in Yangtze River Basin. *Yangtze River* 44(15):11–18 (in Chinese)
- Liang K, Liu S, Bai P, Nie R (2015) The Yellow River basin becomes wetter or drier? The case as indicated by mean precipitation and extremes during 1961–2012. *Theor Appl Climatol* 119(3–4):701–722
- Mann HB (1945) Nonparametric tests against trend. *Econometrica* 13:245–259
- Martin-vide J (2004) Spatial distribution of a daily precipitation concentration index in Peninsular Spain. *Int J Climatol* 24:959–971
- Pettitt AN (1979) A non-parametric approach to the change-point problem. *Appl Stat* 28(2):126–135
- Si D, Ding YH, Liu YJ (2009) Decadal northward shift of the Meiyu belt and the possible cause. *Chin Sci Bull* 54(24):4742–4748
- Su BD, Jiang T, Jin WB (2006) Recent trends in observed temperature and precipitation extremes in the Yangtze River basin, China. *Theor Appl Climatol* 83(1–4):139–151
- Sun JQ, Wang HJ, Yuan W (2009) A possible mechanism for the covariability of the boreal spring Antarctic Oscillation and the Yangtze River valley summer rainfall. *Int J Climatol* 29(9):1276–1284. doi:10.1002/joc.1773
- Sundaram S, Yin QZ, Berger A, Muri H (2012) Impact of ice sheet induced North Atlantic oscillation on East Asian summer monsoon during an interglacial 500,000 years ago. *Clim Dynam* 39(5):1093–1105
- Wang YQ, Zhou L (2005) Observed trends in extreme precipitation events in China during 1961–2001 and the associated changes in large-scale circulation. *Geophys Res Lett* 32, L09707. doi:10.1029/2005GL022574
- Wang J, Jiang ZH, Yan ML, Zhang JL (2008) Trends of extreme precipitation indices in the mid-lower Yangtze River valley of China during 1960–2005. *Sci Meteorol Sin* 28(4):384–388 (in Chinese)
- Wang Q, Zhang MJ, Wang SJ, Ma Q, Sun MP (2014) Changes in temperature extremes in the Yangtze River Basin, 1962–2011. *J Geogr Sci* 24(1):59–75
- Xie ZQ, Du Y, Jiang AJ, Ding YG (2005) Climatic trends of different intensity heavy precipitation events concentration in China. *J Geogr Sci* 15(4):459–466
- Xu ZX, Takeuchi K, Ishidaira H (2003) Monotonic trend and step changes in Japanese precipitation. *J Hydrol* 279(1–4):144–150
- Xu CY, Widden E, Halldin S (2005) Modeling hydrological consequences of climate change—progress and challenge. *Adv Atmos Sci* 22(6):789–797
- You QL, Kang SC, Aguilar E, Pepin N, Flügel WA, Yan YP, Xu YW, Zhang YJ, Huang J (2011) Changes in daily climate extremes in

- China and their connection to the large scale atmospheric circulation during 1961–2003. *Clim Dyn* 36(11–12):2399–2417
- Yu RC, Wang B, Zhou T (2004) Tropospheric cooling and summer monsoon weakening trend over East Asia. *Geophys Res Lett* 31, L22212. doi:[10.1029/2004GL021270](https://doi.org/10.1029/2004GL021270)
- Zhai PM, Zhang XB, Wan H, Pan XH (2005) Trends in total precipitation and frequency of daily precipitation extremes over China. *J Clim* 18: 1096–1108
- Zhang LJ, Qian YF (2003) Annual distribution features of the yearly precipitation in China and their interannual variations. *Acta Meteor Sin* 17(2):146–163
- Zhang XB, Aguilar E, Sensoy S et al (2005) Trends in Middle East climate extreme indices from 1950 to 2003. *J Geophys Res* 110, D22104. doi:[10.1029/2005JD006181](https://doi.org/10.1029/2005JD006181)
- Zhang DQ, Feng GL, Hu JG (2008) Trend of extreme precipitation events over China in last 40 years. *Chinese Phys B* 17(2):736–742
- Zhang Q, Xu CY, Marco G, Chen YP, Liu CL (2009) Changing properties of precipitation concentration in the Pearl River basin, China. *Stoch Environ Res Risk Assess* 23(3):377–385
- Zhang Q, Xu CY, Chen X, Zhang Z (2011) Statistical behaviours of precipitation regimes in China and their links with atmospheric circulation 1960–2005. *Int J Climatol* 31:1665–1678. doi:[10.1002/joc.2193](https://doi.org/10.1002/joc.2193)
- Zhao GJ, Mu XM, Hörmann G, Fohrer N, Xiong M, Su BD, Li XC (2011) Spatial patterns and temporal variability of dryness/wetness in the Yangtze River Basin, China. *Quatern Int* 282(19):5–13